Effect of Different Yield Functions on Computations of Forming Limit Curves for Aluminum Alloy Sheets

F. Mousavi, M. Erfanian, R. Hashemi*, R. Madoliat

[1] S*chool of Mechanical Engineering, Iran University of Science and Technology*.

ARTICLE INFO

Article history:

Received 31 January 2017
Accepted 2 October 2018
Available online 5 November 2018

Keywords:

Forming limit diagram
Aluminum
Yield functions
Marciniak-Kuczynski theory

ABSTRACT

In this article, the effect of different yield functions on the prediction of forming limit diagram (FLD) for the aluminum sheet is studied. Due to the importance of FLD in sheet metal forming, concentration on effective parameters must be considered precisely to have better theoretical prediction comparing experimental results. Yield function is one of the factors that can be improved by adding new coefficients and consequently follows the behaviour of material with good approximation. Therefor applying different yield functions can change shape and level of FLDs. In this study the yield criteria which are used in the determination of forming limit curves, are Hill48, Hosford, BBC2008, Soare2008, Plunkett2008 and Yld2011. The Yld2011 yield function is more appropriate than the other yield functions for prediction of the FLD of aluminum alloy. The well-known Marciniak-Kuczynski (M-K) theory and voce hardening law have also been used. To verify the numerical results, the obtained results have been compared with available experimental data.

1-Introduction

Sheet metal can sustain the limited amount of stretch during forming due to occurrence of localized neck. Forming limit diagram (FLD) is a tool which can be used to detect the initiation of necking [1,2]. Generating FLD with experimental methods needs a lot of time and cost, so obtaining them by theoretical methods with good accuracy is really essential in metal forming. One of the mathematical methods that is useful in generating FLD is Marciniak-Kuczynski (M-K) theory [3,4]. A lot of researches have been done by using this model to consider the effect of different factors consist of anisotropy coefficient, inhomogeneous coefficient, principal strain, strain hardening exponent, strain rate and various yield criteria in predicting FLD [4,5]. Yield function describes the behavior of material, so each type of metal can be described better with a special kind of yield criterion. It means that this yield criterion can predict limit strains more accurately and better predictions of FLDs will be obtained in comparison by experimental ones.

Effect of different yield criteria on the computation of forming limit diagram has been the subject of several researches. For instance, Butut et al. [5] studied the effect of two yield functions, Yld96 and BBC2000, on predicting FLD for orthotropic metal sheets under plane strain condition. Also, they considered effect of anisotropy coefficient on FLD for AA5XXX by M-K model and voce hardening law and by using these two yield functions. Ganjiani and Assempour [6] studied Hosford and BBC2000 in conjunction with the M-K model, they showed that 6th exponent of Hosford yield criterion for AK steel and 8th exponent of Hosford and BBC2000 for AA5XXX were appropriate refer to experimental results. Ahmadi et al. [7] obtained FLD for AA3003-O

* Corresponding author:
E-mail address: rhashemi@iust.ac.ir

by using the M-K model and voce and swift hardening law.
Consequently, they claimed that BBC2003 and the Voce law hardening were suitable for AA3003-O. Yoon et al. [8] obtained FLD for AA5042-H2 by using the anisotropy yield function Yld2000-2D and a form of CPB06ex2 yield function and voce work hardening law. Rezaie bazzaz et al. [9] focused on the effect of strain hardening exponent and strain rate in FLD of IF steel, AA3003-O and AA8014-O by Hill 93 yield criterion.
Consequently, found out increasing these parameters cause more formability. Dasappa et al. [10] reported FLD of AA5754 by using five yield criteria to consist of Hill48, Hill90, Hill93, Yld89 and Plunkett 2008. They achieved that prediction of forming limit diagram strongly related to yield criteria and material parameters. Xiaoqiang et al [11] consider von Mises, Hill48 and Yld89 in the prediction of FLD for Al-Li 2198-T3, and discovered that Hosford yield function for the left side and Hill48 for the right side of the diagram is suitable according to experimental data. Panich et al. [12] studied forming limit stress diagram and forming limit diagram of two kinds of high strength steel, DP780 and TPIR780, which were modeled with von Mises, Hill48 and Yld2000 yield criteria and voce and swift hardening laws. They confirmed that hardening law and yield criterion are effective parameters in the prediction of forming limit diagram. Aretz et al. [13] demonstrated the ability of Yld2011-18p and Yld2011-27p yield functions in describing complex plastic orthotropy of sheet metals. Panich et al. [14] determined experimental FLDs of the AHS steel grade DP980 by the Nakazima stretch-forming test. Then, theoretical FLDs according to the M-K model were calculated using the Swift hardening law coupled with the Yld2000-2d, Yld89 stress based, Yld89 strain based, Hill'48 stress based and Hill'48 strain based yield criteria.
These days, aluminum alloys are used a lot in sheet forming industry. Therefore, having enough information around formability of them is essential. One of the useful applications in this field is forming limit diagram. Due to lack of suitable implementation of classic yield function such as von Mises and Hill's 48 to determine the anisotropy plastic behavior and FLDs for aluminum alloy sheet metals particularly, the advanced yield criterion was introduced to obtain satisfactory accuracy and agreement between the theoretical and experimental results.
In this research, the effect of several yield functions (e.g., Hill48, Hosford, BBC2008, Soare2008, Plunkett2008 and Yld2011) on the prediction of forming limit diagrams for the five kinds of aluminum alloy sheets are determined. The methodology for computation of the FLDs is based on the well-known M-K theory and the Voce hardening law is also considered. Consequently, the Yld2011 yield criterion approximately describes the forming behavior of aluminum sheet more accurately.

2-The Marciniak-Kuczynski model

In the M-K model assumes that there is an initial defect on a sheet surface. A narrow groove inclined at an angle of θ respect to the principal axis causes an inhomogeneous factor which leads to necking. This inhomogeneity maybe is the result of surface or different mechanical properties of the material in the different regions [4]. The M-K analysis schematically illustrated in figure 1.

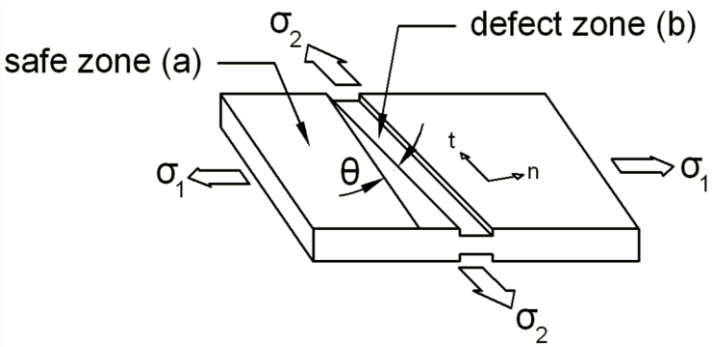

Fig.1. The schematic of M-K model.

The M-K model supposes that the sheet has two regions: 1- homogeneous or safe region (a) and t_0^a is the initial thickness of this zone, 2- inhomogeneous or groove region with initial thickness shown as t_0^b. It is necessary to state that x, y, z -axes correspond to rolling, transverse and normal sheet's directions, whereas 1 and 2 show the principal stress and strain directions in homogeneous region and the groove region the axis represent by n, t, z. The initial geometrical inhomogeneity is reported as an initial defect factor that is shown by f_0 and characterized as the following form:

$$f_0 = (\frac{t_a}{t_b}) \tag{1}$$

During plastic deformation, this defect factor changes respect to below relation and shows this factor is a function of the initial defect:

$$f = \frac{t^b}{t^a} = f_0 * \exp\left(\epsilon^b{}_3 - \epsilon^a{}_3\right) \tag{2}$$

In above relation, ϵ_3 refers to strain along thickness direction and calculated by relation which is consisting of incompressibility condition:

$$\epsilon_3 = -(\epsilon_1 + \epsilon_2) \tag{3}$$

It is assumed that strains along the groove direction are equal in two regions also during deformation process, strain ratio which is defined as minimum strain to maximum strain inside the groove region decreases and in the outside region of groove is constant (proportional deformation). It can be claimed that the groove deformation is close to plane strain condition. By this condition, stress and strain increments of groove zone can directly obtained respect to their value in safe zone. The main equations in the M-K model generate from equilibrium and compatibility equations. For finding the value of limit strains and stresses it is assumed that the stress ratio, $\frac{\sigma^a{}_1}{\sigma^a{}_2}$, is constant. At first step, all the strains are zero and the loading on the safe zone started by assuming a small value for $d\bar{\epsilon}^a$ (for instance $d\bar{\epsilon}^a$=0.0001) and the equivalent strain, $\bar{\epsilon}^a$, will be calculated.

$$\bar{\epsilon}^a|_{new} = \bar{\epsilon}^a|_{new} + d\bar{\epsilon}^a \tag{4}$$

The effective stress, $\bar{\sigma}_Y$, is obtained by substituting the effective strain in the hardening law. It is clear that the effective stresses which are obtained from hardening law are equal to those obtaining by yield function. Using the assumed $d\bar{\epsilon}^a$ in the flow rule, stress and strain components in the safe zone are calculated and after that by using rotation matrix, T, the stress and strain tensors are transformed to groove coordinates using equations (5) and (6).

$$T = \begin{bmatrix} \cos\theta & \sin\theta \\ -\sin\theta & \cos\theta \end{bmatrix} \tag{5}$$

$$\sigma^{\mathrm{ntz}} = T\sigma^{\mathrm{xyz}}\mathrm{T}^{\mathrm{T}} = \begin{bmatrix} \sigma_{\mathrm{nn}} & \sigma_{\mathrm{nt}} \\ \sigma_{\mathrm{nt}} & \sigma_{\mathrm{tt}} \end{bmatrix} \tag{6}$$

After calculation of safe zone's stress and strain components, same variables must be calculated in the groove zone. Unknown parameters in groove region consist of $d\epsilon^b{}_{tt}$, $d\epsilon^b{}_{nt}$, $d\epsilon^b{}_{nn}$, $\sigma^b{}_{nn}$, $\sigma^b{}_{tt}$, $\sigma^b{}_{nt}$ stress increments are functions of $d\bar{\epsilon}^b$, $\sigma^b{}_{tt}$, $\sigma^b{}_{nn}$ and $\sigma^b{}_{nt}$. So, the unknown parameters in this zone reduced to four parameters ($d\bar{\epsilon}^b$, $\sigma^b{}_{nn}$, $\sigma^b{}_{tt}$ and $\sigma^b{}_{nt}$). The force equilibrium equations in the groove's normal and tangential directions can be written as follows:

$$F_{nn}{}^b = F_{nn}{}^a \tag{7}$$

$$F_{nt}{}^b = F_{nt}{}^a \tag{8}$$

Changes that related to thickness in each step can be expressed as a function of thickness strain.

$$t^a = t^a{}_0 * \exp\left(\epsilon^a{}_3\right) \tag{9}$$

$$t^b = t^b{}_0 * \exp\left(\epsilon^b{}_3\right) \tag{10}$$

From equation (7) and (8) the force equilibrium equations can be written as below forms:

$$f\sigma^b{}_{nn} = \sigma^b{}_{nn} \tag{11}$$

$$f\sigma^b{}_{nt} = \sigma^a{}_{nt} \tag{12}$$

Refer to compatibility equation, elongation in both regions is equal:

$$d\varepsilon_{tt}{}^{b} = d\varepsilon_{tt}{}^{a} \quad (13)$$

Finally, the energy equilibrium relation written as follows:

$$d\epsilon^{b}{}_{nn}\sigma^{b}{}_{nn} + d\epsilon^{b}{}_{tt}\sigma^{b}{}_{tt} + d\epsilon^{b}{}_{nt}\sigma^{b}{}_{nt} = d\bar{\varepsilon}^{b}\bar{\sigma}_{Y}{}^{b} \quad (14)$$

In equation (11), $\bar{\sigma}_{Y}{}^{b}$, is the effective stress of groove zone that obtained by hardening law. So three equations obtained from compatibility and force equilibrium conditions and one other equation from energy relation generated. These four non-linear equations are as follows:

$$F_1 = \frac{d\varepsilon_{nn}{}^{b}\sigma_{nn}{}^{b} + d\varepsilon_{tt}{}^{b}\sigma_{tt}{}^{b} + d\varepsilon_{nt}{}^{b}\sigma_{nt}{}^{b}}{d\bar{\varepsilon}^{b}\bar{\sigma}_{Y}{}^{b}} - 1 = 0 \quad (15)$$

$$F_2 = \frac{d\varepsilon_{tt}{}^{b}}{d\varepsilon_{tt}{}^{a}} - 1 = 0 \quad (16)$$

$$F_3 = f\frac{\sigma_{nn}{}^{b}}{\sigma_{nn}{}^{a}} - 1 = 0 \quad (17)$$

$$F_4 = f\frac{\sigma_{nt}{}^{b}}{\sigma_{nt}{}^{a}} - 1 = 0 \quad (18)$$

The unknown parameters and functions can be defined as two vectors called X and F and come at below:

$$[x] = [\sigma^{b}{}_{tt}\ \sigma^{b}{}_{nn}\ \sigma^{b}{}_{nt}\ d\epsilon^{b}]^{T} \quad (19)$$

$$[F] = [F_1\ \ F_2\ \ F_3\ \ F_4]^{T} \quad (20)$$

In order to solve this non-linear system of equations and calculating the unknown parameters of the groove zone, the Newton-Raphson method is applied. The general procedure of this method explained in following. The goal is solving system of equations which include N functional relations and each relation has N variables:

$$F_i(x_1, x_2, \dots\dots, x_N) = 0 \quad i = 0, 1, 2, \dots,, N \quad (21)$$

In the neighborhood of x, each function can be expanded in Taylor series as follows:

$$F_i(\mathrm{x} + \delta\mathrm{x}) = F_i(x) + \sum_{j=1}^{N}\frac{\partial F_i}{\partial x_j}\delta x_j + \mathrm{O}(\delta x^2) \quad (22)$$

In equation (22), $\frac{\partial F_i}{\partial x_j}$ terms are the components of Jacobian matrix:

$$J_{ij} = \frac{\partial F_i}{\partial x_j} \quad (23)$$

So relation (22) can be rewritten in below form:

$$F(\mathrm{x} + \delta\mathrm{x}) = F(x) + J, \delta x + \mathrm{O}(\delta x^2) \quad (24)$$

By neglecting terms of order 2 or higher and considering F (x+δx) = 0 it is obtained:

$$J, \delta x = -F \quad (25)$$

$$\delta\mathrm{x} = -J^{-1}, F \quad (26)$$

Another equation shows the relation of the variable, x, in two consecutive steps:

$$x_{new} = x_{old} + \lambda\delta\mathrm{x} \quad (27)$$

By using backtracking algorithm an acceptable newton step length, λ, can be found. Value of this parameter is effective in convergence behavior of the Newton-Raphson method.
The Jacobian matrix of four non-linear equations system defined as follow:

$$J = \begin{bmatrix} \frac{\partial F_1}{\partial\sigma^{b}{}_{nn}} & \frac{\partial F_1}{\partial\sigma^{b}{}_{tt}} & \frac{\partial F_1}{\partial\sigma^{b}{}_{nt}} & \frac{\partial F_1}{d\bar{\epsilon}^{b}} \\ \frac{\partial F_2}{\partial\sigma^{b}{}_{nn}} & \frac{\partial F_2}{\partial\sigma^{b}{}_{tt}} & \frac{\partial F_2}{\partial\sigma^{b}{}_{nt}} & \frac{\partial F_2}{d\bar{\epsilon}^{b}} \\ \frac{\partial F_2}{\partial\sigma^{b}{}_{nn}} & \frac{\partial F_2}{\partial\sigma^{b}{}_{tt}} & \frac{\partial F_2}{\partial\sigma^{b}{}_{nt}} & \frac{\partial F_2}{d\bar{\epsilon}^{b}} \\ \frac{\partial F_2}{\partial\sigma^{b}{}_{nn}} & \frac{\partial F_2}{\partial\sigma^{b}{}_{tt}} & \frac{\partial F_2}{\partial\sigma^{b}{}_{nt}} & \frac{\partial F_2}{d\bar{\epsilon}^{b}} \end{bmatrix} \quad (28)$$

The M-K model assumes that necking localization occurs when the equivalent strain in the groove region ($d\bar{\epsilon}^{b}$) is 10 times greater than in homogeneous zone ($d\bar{\epsilon}^{a}$), so when the necking criterion occurs, the corresponding strains ($\epsilon^{a}{}_{xx}, \epsilon^{a}{}_{yy}$) accumulated at that moment in the homogeneous zone are the limit strains. The process is repeated for different value of θ between 0 and 90 and minimum value of the major strain is selected as a limit point on the FLD. All steps are repeated by choosing another stress ratio, and obtained set of strains for each value of α are used for plotting the FLD.

3-Advanced Yield functions

One of the factors that describe the behavior of metals is the yield criterion. So it has an excessive effect on FLD's accuracy. A yield surface is generally described by an implicit relation of the below form:

$$\varphi(\bar{\sigma},\mathrm{Y}) := \bar{\sigma} - \mathrm{Y} = 0 \tag{29}$$

where $\bar{\sigma}$ is the equivalent stress and Y the yield parameter which is obtained by a simple tension, compressor or cutting test. The yield surface is the locus of stresses in which the material behavior changes from elastic to plastic condition. Yield function is a mathematical expression of this locus which is consisting of six stress components (3 of normal stresses and 3 of shear stresses). Different yield criteria considered during recent years in order to have better matching with experimental results. A brief description of each model that considered in this research summarized here.

3-1- Hill's 1948 yield function

A well-known quadratic anisotropic yield criterion proposed by Hill [15] is one of the most widely recognized yield functions. Hill 48 yield function is the advanced form of von Mises that can follow anisotropic behavior of metals. This yield criterion is represented by:

$$\bar{\sigma}_y = \sqrt{\frac{1}{2}\bar{\sigma}^T : M : \bar{\sigma}} = \sqrt{\frac{1}{2}[(G+H)\sigma_{xx}{}^2 - 2H\sigma_{xx}\sigma_{yy} + (F+H)\sigma_{yy}{}^2 + 2N\sigma_{xy}{}^2} \tag{30}$$

The above relation is in plane stress state (σ_{zz}, σ_{zx}, σ_{zy}= 0) where F, G, H and N are the anisotropic material coefficients and can be formulated in terms of the r-values r_0, r_{45}, r_{90} as follows:

$$F = \frac{2r_0}{r_{90}(1+r_{45})}\ , G = \frac{2}{1+r_0}\ ,\quad N = \frac{(r_0+r_{90})(2r_{45}+1)}{r_{90}(1+r_0)}\ ,\quad \mathrm{H} = \frac{r_0}{(1+r_0)} \tag{31}$$

3-2- Hosford yield criterion

Hosford yield criterion in plane stress state is as following form:

$$\bar{\sigma}_y = \frac{1}{[r_{90}(1+r_0)]^{\frac{1}{a}}}(r_{90}|\sigma_1|^a + r_0|\sigma_2|^a + r_0 r_{90}|\sigma_1 - \sigma_2|^a)^{\frac{1}{a}} \tag{32}$$

The essential difference between the approaches by Hosford and Hill consist in the different ways of determining the exponent "a". Hosford related "a" to the crystallographic structure of the material. He concluded that the best approximation was given by a=6 for BCC materials and a=8 for FCC materials [16].

3-3- BBC2008 yield function

In order to enhance the flexibility of the BBC yield criterion, a new version of this model has been developed. The model is expressed as a finite series (using 8 or 16 material parameter) that can be expanded to retain more or less terms, depending on the volume of experimental data. This equation is as follows [17]:

$$\frac{\bar{\sigma}^{2k}}{\mathrm{w}-1} = \sum_{\mathrm{i}=1}^{\mathrm{s}} \{\mathrm{w}^{\mathrm{i}-1}\{[\mathrm{L}^{(\mathrm{i})} + \mathrm{M}^{(\mathrm{i})}]^{2\mathrm{k}} + [\mathrm{L}^{(\mathrm{i})} - \mathrm{M}^{(\mathrm{i})}]^{2\mathrm{k}}\} + w^{s-1}\{[M^{(i)} + N^{(i)}]^{2k} + [M^{(i)} - N^{(i)}]^{2\mathrm{k}}\}\} \tag{33}$$

$$w = (3/2)^{\frac{1}{s}} > 1$$

$$\mathrm{L}^{(\mathrm{i})} = l_1{}^{(\mathrm{i})}\sigma_{11} + \mathrm{l}_2{}^{(\mathrm{i})}\sigma_{22}$$

$$\mathrm{M}^{(\mathrm{i})} = \sqrt{[\mathrm{m}_1{}^{(\mathrm{i})}\sigma_{11} - \mathrm{m}_2{}^{(\mathrm{i})}\sigma_{22}]^2 + [\mathrm{m}_3{}^{(\mathrm{i})}(\sigma_{12}+\sigma_{21})]^2}$$

$$\mathrm{N}^{(\mathrm{i})} = \sqrt{[\mathrm{n}_1{}^{(\mathrm{i})}\sigma_{11} - \mathrm{n}_2{}^{(\mathrm{i})}\sigma_{22}]^2 + [\mathrm{n}_3{}^{(\mathrm{i})}(\sigma_{12}+\sigma_{21})]^2} \tag{34}$$

When s=1 this yield criterion shown as BBC2008-8 parameters and for s=2, BBC 2008-16 parameters. Also k=3 for BBC material and k=4 for FCC structure of them are suitable and $l_1{}^{(\mathrm{i})}, \mathrm{l}_2{}^{(\mathrm{i})}, \mathrm{m}_1{}^{(\mathrm{i})}, \mathrm{m}_2{}^{(\mathrm{i})}, \mathrm{m}_3{}^{(\mathrm{i})}, \mathrm{n}_1{}^{(\mathrm{i})}, \mathrm{n}_2{}^{(\mathrm{i})}, \mathrm{n}_3{}^{(\mathrm{i})}$ are the materials parameter.

3-4- Soare2008 yield function

The quadratic polynomial yield functions cannot achieve a completely satisfactorily description for some materials. Soare criterion introduced higher order polynomials of order 4, 6 and 8. Assuming plane stress state these yield functions are as follows [18]:

$$\mathrm{P}_4 = \mathrm{a}_1\sigma_x{}^4 + \mathrm{a}_2\sigma_x{}^3\sigma_y + \mathrm{a}_3\sigma_x{}^2\sigma_y{}^2 + \mathrm{a}_4\sigma_x\sigma_y{}^3 + \mathrm{a}_5\sigma_y{}^4 + (\mathrm{a}_6\sigma_x{}^2 + \mathrm{a}_7\sigma_x\sigma_y + \mathrm{a}_8\sigma_y{}^2)\sigma_{xy}{}^2 + \mathrm{a}_9\sigma_{xy}{}^4 \tag{35}$$

$$\mathrm{P}_6 = \mathrm{a}_1\sigma_x{}^6 + \mathrm{a}_2\sigma_x{}^5\sigma_y + \mathrm{a}_3\sigma_x{}^4\sigma_y{}^2 + \mathrm{a}_4\sigma_x{}^3\sigma_y{}^3 + \mathrm{a}_5\sigma_x{}^2\sigma_y{}^4 + \mathrm{a}_6\sigma_x\sigma_y{}^5 + \mathrm{a}_7\sigma_y{}^6 + (\mathrm{a}_8\sigma_x{}^4 + \mathrm{a}_9\sigma_x{}^3\sigma_y + \mathrm{a}_{10}\sigma_x{}^2\sigma_y{}^2 + \mathrm{a}_{11}\sigma_x\sigma_y{}^3 + \mathrm{a}_{12}\sigma_y{}^4)\sigma_{xy}{}^2 + (\mathrm{a}_{13}\sigma_x{}^2 + \mathrm{a}_{14}\sigma_x\sigma_y + \mathrm{a}_{15}\sigma_y{}^2)\sigma_{xy}{}^4 + \mathrm{a}_{16}\sigma_{xy}{}^4 \tag{36}$$

$$P_8 = a_1\sigma_x^8 + a_2\sigma_x^7\sigma_y + a_3\sigma_x^6\sigma_y^2 + a_4\sigma_x^5\sigma_y^3 + a_5\sigma_x^4\sigma_y^4 + a_6\sigma_x^3\sigma_y^5 + a_7\sigma_x^2\sigma_y^6 + a_8\sigma_x\sigma_y^7 + a_9\sigma_y^8 + \left(a_{10}\sigma_x^6 + a_{11}\sigma_x^5\sigma_y + a_{12}\sigma_x^4\sigma_y^2 + a_{13}\sigma_x^3\sigma_y^3 + a_{14}\sigma_x^2\sigma_y^4 + a_{14}\sigma_x^2\sigma_y^4 \quad a_{16}\sigma_y^6\right)\sigma_{xy}^2 + \left(a_{17}\sigma_x^4 + a_{18}\sigma_x^3\sigma_y + a_{19}\sigma_x^2\sigma_y^2 + a_{20}\sigma_x\sigma_y^3 + a_{21}\sigma_y^4\right)\sigma_{xy}^4 + \left(a_{22}\sigma_x^2 + a_{23}\sigma_x\sigma_y + a_{24}\sigma_y^2\right)\sigma_{xy}^6 + a_{25}\sigma_{xy}^8 \quad (37)$$

In relations (32), (33) and (34), a_i are material parameters.

3-5- Plunkett2008 yield function

Plunkett et al. define CPB06 yield criterion to describe the orthotropic metal sheet behavior. In this criterion, anisotropy is obtained by linear transformation of deviatory stress tensor. It can predict tension/compression state for HCP and FCC structural material with good accuracy. The yield functions with two, three and four linear transformation are shown as CPB06ex4, CPB06ex2 and CPB06ex6 [19].

Following relation is CPB06ex2 yield function:

$$F(\Sigma, \acute{\Sigma}, k, \acute{k}, a) = (|\Sigma_1| - k\Sigma_1)^a + (|\Sigma_2| - k\Sigma_2)^a + (|\Sigma_3| - k\Sigma_3)^a + (|\acute{\Sigma}_1| - \acute{k}\acute{\Sigma}_1)^a + (|\acute{\Sigma}_2| - \acute{k}\acute{\Sigma}_2)^a + (|\acute{\Sigma}_3| - \acute{k}\acute{\Sigma}_3)^a \quad (38)$$

Where k and k′ are the material parameters for description of strength differential effects, and "a" is the degree of homogeneity, ($\Sigma_1, \Sigma_2, \Sigma_3$) and ($\acute{\Sigma}_1, \acute{\Sigma}_2, \acute{\Sigma}_3$) are the basic value of transformed stress tensors. The linear transformation of deviatory stress tensor, S, defined as follows:

$$\Sigma = C:S \quad , \quad \acute{\Sigma} = \acute{C}:\acute{S} \quad (39)$$

The fourth-order tensors, C and C' operating on the stress deviator is represented by:

$$C=\begin{bmatrix} C_{11} & C_{12} & C_{13} & 0 & 0 & 0 \\ C_{12} & C_{22} & C_{23} & 0 & 0 & 0 \\ C_{13} & C_{23} & C_{33} & 0 & 0 & 0 \\ 0 & 0 & 0 & C_{44} & 0 & 0 \\ 0 & 0 & 0 & 0 & C_{55} & 0 \\ 0 & 0 & 0 & 0 & 0 & C_{66} \end{bmatrix} \quad (40)$$

$$\acute{C}=\begin{bmatrix} \acute{C}_{11} & \acute{C}_{12} & \acute{C}_{13} & 0 & 0 & 0 \\ \acute{C}_{12} & \acute{C}_{22} & \acute{C}_{23} & 0 & 0 & 0 \\ \acute{C}_{13} & \acute{C}_{23} & \acute{C}_{33} & 0 & 0 & 0 \\ 0 & 0 & 0 & \acute{C}_{44} & 0 & 0 \\ 0 & 0 & 0 & 0 & \acute{C}_{55} & 0 \\ 0 & 0 & 0 & 0 & 0 & \acute{C}_{66} \end{bmatrix} \quad (41)$$

CPB06ex2 is used in this article named as Plunkett 2008.

3-6-Yld2011 yield function

This yield criterion describes orthotropic metal sheets and has two types; one is calibrated by 18 parameters and named Yld2011-18p. Another one calibrated by 27 parameters and called Yld2011-27p. This yield function describes stress in 3 dimensions and presented by Aretz and Barlat [13]. The advantage of that is easy application of this yield criterion in finite element code. Yld2011-18p with two linear transformations is defined as follows:

$$\bar{\sigma} = \left\{\frac{1}{\xi}\left[\sum_{i=1}^{3}\sum_{j=1}^{3}|\dot{S}_i + \ddot{S}_j|^m\right]\right\}^{1/m} \quad (42)$$

$$= \left\{\frac{1}{\xi}\left[|\dot{S}_1 + \ddot{S}_1|^m + |\dot{S}_1 + \ddot{S}_2|^m + |\dot{S}_1 + \ddot{S}_3|^m + |\dot{S}_2 + \ddot{S}_1|^m + |\dot{S}_2 + \ddot{S}_2|^m + |\dot{S}_2 + \ddot{S}_3|^m + |\dot{S}_3 + \ddot{S}_1|^m + |\dot{S}_3 + \ddot{S}_2|^m + |\dot{S}_3 + \ddot{S}_3|^m\right]\right\}^{1/m}$$

Also ξ in equation (3-42) is as the following form:

$$\xi = \left(\frac{4}{3}\right)^m + 4\left(\frac{2}{3}\right)^m + 4\left(\frac{1}{3}\right)^m \quad , \quad m \geq 1 \quad (43)$$

By adding a third linear transformation, Yld2011-27p obtained and its equivalent stress is defined as follows:

$$\bar{\sigma} = \left\{\frac{1}{\xi}\left[\sum_{i=1}^{3}\sum_{j=1}^{3}|\dot{S}_i + \ddot{S}_j|^m + \sum_{j=1}^{3}|\dddot{S}_i|^m\right]\right\}^{1/m} \quad (44)$$

And:

$$\xi = \left(\frac{4}{3}\right)^m + 5\left(\frac{2}{3}\right)^m + 6\left(\frac{1}{3}\right)^m \quad , \quad m \geq 1 \quad (45)$$

In the above relation, the transformation defined as follows:

$$\acute{S} = \acute{C}:S \quad (47)$$

$$\begin{bmatrix} \acute{S}_{11} \\ \acute{S}_{22} \\ \acute{S}_{33} \\ \acute{S}_{32} \\ \acute{S}_{31} \\ \acute{S}_{12} \end{bmatrix} = \begin{bmatrix} 0 & -\acute{C}_{12} & \acute{C}_{13} & 0 & 0 & 0 \\ -\acute{C}_{12} & 0 & -\acute{C}_{23} & 0 & 0 & 0 \\ -\acute{C}_{13} & -\acute{C}_{23} & 0 & 0 & 0 & 0 \\ 0 & 0 & 0 & \acute{C}_{44} & 0 & 0 \\ 0 & 0 & 0 & 0 & \acute{C}_{55} & 0 \\ 0 & 0 & 0 & 0 & 0 & \acute{C}_{66} \end{bmatrix} \begin{bmatrix} S_{11} \\ S_{22} \\ S_{33} \\ S_{32} \\ S_{31} \\ S_{21} \end{bmatrix}$$

4-Results and discussion

4-1-Forming limit diagrams of aluminum alloy

In this part, to compare the flexibility of different yield functions in describing the formability of different aluminum sheets, the forming limit diagrams are determined by using Hill 48, Hosford, BBC2008, Soare 2008, Plunkett2008 and Yld2011. The Voce hardening law is considered in this article. Finally, the

theoretical FLDs are compared to the experimental results and the effect of yield criteria on the prediction of the FLDs is investigated.

4-1-1-AA2090-T3 alloy

This alloy examined in this article and forming limit diagram is obtained by considering the voce hardening law and the yield criteria explained in the last part. The initial defect factor is assumed as f_0= 0.995. The mechanical properties and anisotropy data are listed in table 1 and the parameters of yield criterions are listed in tables 2 to 5.

Table 1. Mechanical properties of Aluminum alloy AA2090-T3 [17].

K[Mpa]	ε_0	n	r_0	r_{45}	r_{90}
646	0.025	0.227	0.21	1.58	0.91

Table 2. BBC 2008 coefficient for aluminium alloy AA2090-T3 [17].

K	s	w	$l_1^{(1)}$	$l_2^{(1)}$	$m_1^{(1)}$	$m_2^{(1)}$	$m_3^{(1)}$
4	2	1.2247	0.1309	0.6217	0.7834	0.6604	0.000079
$n_1^{(1)}$	$n_2^{(1)}$	$n_3^{(1)}$	$l_1^{(2)}$	$l_2^{(2)}$	$m_1^{(2)}$	$m_2^{(2)}$	$m_3^{(2)}$
0.111	0.0482	0.3075	1.0339	-0.0720	0.000113	0.000077	0.5380
$n_1^{(2)}$	$n_2^{(2)}$	$n_3^{(2)}$					
0.0558	1.0186	0.7781					

Table 3. Soare 2008 coefficient of aluminum alloy AA2090-T3 [18].

a_1	a_2	a_3	a_4	a_5	a_6	a_7	a_8
1	-1.1059	2.5255	-5.1914	6.1458	-4.3254	1.7753	14.190
a_9	a_{10}	a_{11}	a_{12}	a_{13}	a_{14}	a_{15}	a_{16}
-4.9759	-4.3926	3.4652	15.806	0	-9.4916	86.661	116.42

Table 5. Yld2011 coefficient of aluminum alloy AA2090-T3 (m=12) [13].

c'_{12}	c'_{13}	c'_{21}	c'_{23}	c'_{31}	c'_{32}	c'_{44}	c'_{55}	c'_{66}
0.44160	-1.18740	0.978656	1.80125	-1.7401	-0.959446	1	1	1.41126
c''_{12}	c''_{13}	c''_{21}	c''_{23}	c''_{31}	c''_{32}	c''_{44}	c''_{55}	c''_{66}
0.7927	0.670733	0.622929	0.6655	0.962866	-0.232442	1	1	1.36

Effect of different yield criteria in predicting FLD of aluminum alloy AA2090-T3 is considered. As illustrated in figure 2 all yield functions capture the trend of experimental FLD correctly, however, in right-hand side the trend is better matched with Yld2011 criterion. Performances of different yield functions in predicting FLD are comparing to each other according to equation (48) listed in table 6. In order to investigate entire curve, 3 different strain ratio (one in left, one in cusp and one in right) is selected in experimental curve and percentage error of counterpart point in each theoretical curve is calculated. It is observed that Yld2011 predicts FLD with good accuracy.

$$\text{percentage error} = \left(\frac{\text{predicred } \epsilon_1 - \text{experimental } \epsilon_1}{\text{experimental } \epsilon_1}\right) \times 100 \quad (48)$$

Reminded that the voce hardening law is as following formula [21]:

$$\bar{\sigma}_y = A - B(\exp(-C\epsilon)) \quad (49)$$

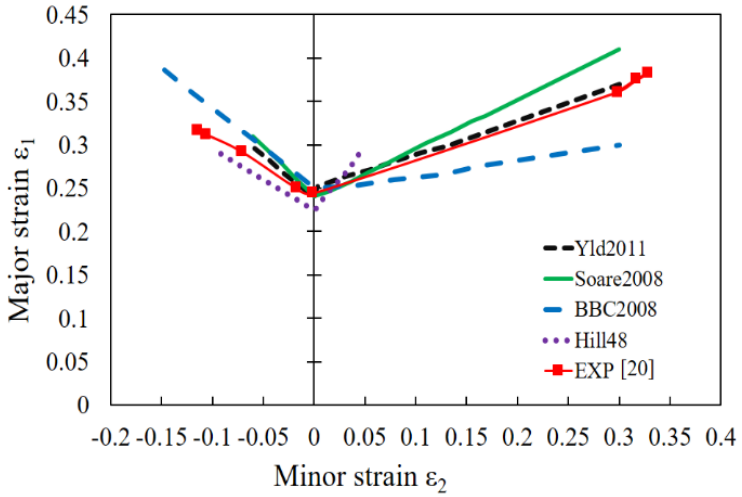

Fig.2. The predicted FLDs for aluminum alloy AA2090-T3.

Table 6. Performance of different yield functions in predicting FLD of AA2090-T3 (in three strain ratios)

	BBC2008	Soare2008	Yld2011	Hill48
-1/3	10	13	6	6
0	0	0	0	7
1	16	12	2	>30

4-1-2- AA5042-H2 alloy

The mechanical and anisotropy data are depicted in table 7 and the instant coefficient of this alloy for Plunkett 2008 and BBC2008 yield criterion are documented in tables 8 and 9. By using voce hardening law, f_0= 0.995 and BBC2008 and Plunkett 2008 yield criterion, FLDs have been obtained and shown in figure 3. As depicted in this figure shows that, Plunkett 2008 predicted the higher level of FLD than BBC.

Table 7. Mechanical properties of aluminum alloy AA5042-H2 [21].

A	B	C	r_0	r_{45}	r_{90}
404.16	107.17	18.416	0.354	1.069	1.396

Table 8. BBC 2008 coefficient for aluminum alloy AA5042-H2 [17].

K	s	w	$l_1^{(1)}$	$l_2^{(1)}$	$m_1^{(1)}$	$m_2^{(1)}$	$m_3^{(1)}$
4	2	1.2247	0.3527	-0.7187	0	0	-0.8769
$n_1^{(1)}$	$n_2^{(1)}$	$n_3^{(1)}$	$l_1^{(2)}$	$l_2^{(2)}$	$m_1^{(2)}$	$m_2^{(2)}$	$m_3^{(2)}$
-0.4479	-0.0714	-0.2061	0.7275	0.3431	-0.5720	-0.6217	0.5675
$n_1^{(2)}$	$n_2^{(2)}$	$n_3^{(2)}$					
-0.2992	-0.6359	0					

Table 9. Plunkett 2008 coefficient of aluminum alloy AA5042-H2 (a=12) [8].

c_{12}	c_{13}	c_{22}	c_{23}	c_{33}	c_{66}
-0.0272	-0.6011	1.2870	0.6864	-0.2736	1.1514
c'_{12}	c'_{13}	c'_{22}	c'_{23}	c'_{33}	c'_{66}
-0.0897	0.0112	1.1322	-0.1092	-1.2009	1.3093

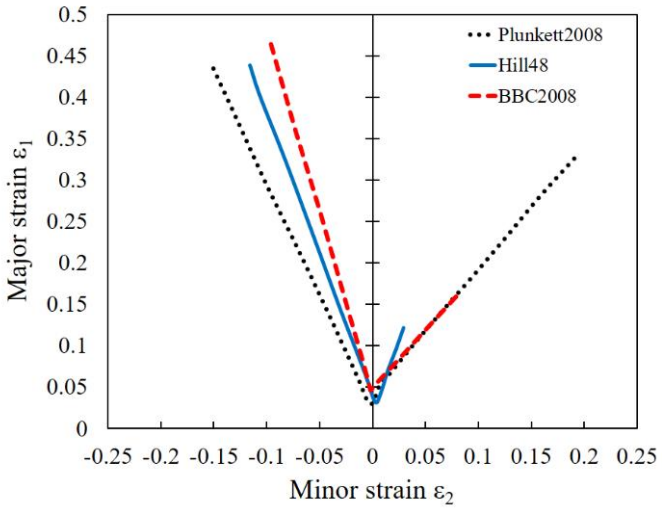

Fig. 3. The predicted FLDs for aluminum alloy AA5042-H2.

4-1-3- AA5754 alloy

Mechanical coefficients of this alloy are summarized in table 10 and the coefficients of Plunkett2008 yield function are listed in table 11. The voce hardening law has been used and its constants gained by curve fitting [10]. Also f_0= 0.985. The effect of Plunkett yield criterion is considered in the prediction of FLD and compared with experimental results. Figure 4 shows the schematic results. Based on this yield criterion the remarkable difference between the theoretical prediction curve and experimental data can be observed in the tension-compression strain states described in the left-hand side of the FLD. But it predicts right-hand side of the FLD with good accuracy.

Table 10. Mechanical properties of aluminum alloy AA5754 [10,22].

A	B	C	r_0	r_{45}	r_{90}
248	160	22.46	0.81	0.58	1.08

Table 11. Plunkett 2008 coefficient of aluminum alloy AA5754 [22].

c_{12}	c_{13}	c_{22}	c_{23}	c_{33}	c_{66}
-0.0272	-0.6011	1.2870	0.6864	-0.2736	1.1514
c'_{12}	c'_{13}	c'_{22}	c'_{23}	c'_{33}	c'_{66}
-0.0897	0.0112	1.1322	-0.1092	-1.2009	1.3093

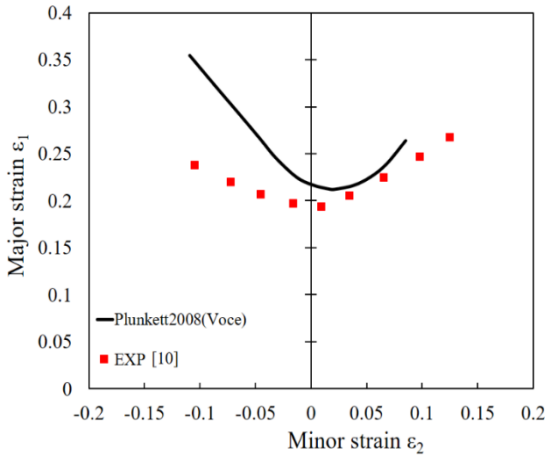

Fig. 4. The predicted FLDs for aluminum alloy AA5754.

4-1-4- AA3104-H19 alloy

Mechanical data of this alloy are summarized in table 12 and the instant coefficient of Yld2011 yield function are in table 13. The predicted forming limit diagram has been shown in figure 5. This diagram is obtained by using voce hardening law [13] and Yld2011 yield criterion and predicted results compared by some experimental data [23]. Due to the lack of experimental data for the right-hand side of FLD, validation is performed only on the left side and around plane strain mode. It can be seen that the Yld2011 yield function predicted results with good accuracy.

Table 12. Mechanical properties of aluminum alloy AA3104-H19 [13].

A	B	C	r_0	r_{45}	r_{90}
263	266	425.8	0.408	0.984	1.416

Table 13. Yld2011 coefficient of aluminum alloy AA3104-H19 (m=12) [13].

c'_{12}	c'_{13}	c'_{21}	c'_{23}	c'_{31}	c'_{32}	c'_{44}	c'_{55}	c'_{66}
1.28025	0.853723	0.758983	1.50001	1.6318	1.45339	1	1	0.880608
c''_{12}	c''_{13}	c''_{21}	c''_{23}	c''_{31}	c''_{32}	c''_{44}	c''_{55}	c''_{66}
0.795767	0.715288	1.18774	0.315233	-0.0608724	0.693975	1	1	1.19887

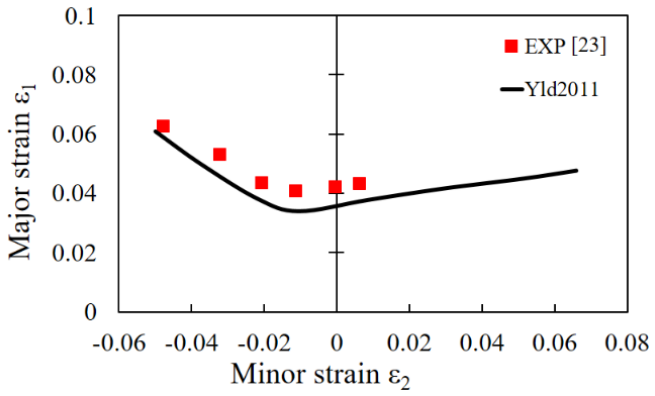

Fig. 5. The predicted FLDs for aluminum alloy AA3104-H19.

4-1-4- AA3003-O alloy

By using experimental data [7], Yld2011-16p and BBC2008 are calibrated, and the instant coefficients are identified. For calibration of a yield criterion some experimental results are necessary. For instance the yield functions σ_φ and anisotropy coefficients r_φ in different directions which are gained by simple tension tests. Also the equibiaxial yield stress σ_b and r-values r_b can be used for this purpose. In this article the experimental data extracted from some tension tests which had performed in 5 different directions, 0, 22.5, 45, 67.5 and 90 to the original rolling direction. Furthermore, an error function (objective function) is created. This function consists of summation of the squares of the errors defined from a comparison between the results obtained from the constitutive equations for a given set of parameters to be identified and the corresponding experimental values. This kind of procedure can be considered as a generalization of the optimization procedure proposed by Banabic [24-25]. The general equation of the error function is as below form in equation (49): where $\sigma^{exp}{}_\varphi$ and $r^{exp}{}_\varphi$ are the experimental yield stresses and anisotropy values obtained by uniaxial tethe nsile test in different directions φ with the rolling direction. Also, $\sigma^{exp}{}_b$ and $r^{exp}{}_b$ are the experimental yield stresses and anisotropy values obtained from the equibiaxal tensile test [27]. The experimental data of the tensile test in 5 different directions are presented in table 14.

Table 14. Experimental values of the material for AA3003-O.

σ_0	$\sigma_{22.5}$	σ_{45}	$\sigma_{67.5}$	σ_{90}
107.3	112.7	116.7	111.3	107.7
r_0	$r_{22.5}$	r_{45}	$r_{67.5}$	r_{90}
0.836	0.605	0.522	0.570	0.594

These data are substituted in the error function as experimental terms and then the error function has to be minimized. To minimization, there are a lot of algorithms that reflect out this approach. The used algorithm in this article is the Genetic Algorithm (GA) which is a selective random search algorithm to achieve a global optimum within a large space of solutions proposed by Holland [26]. In this work the coefficients of BBC2008 and Yld2011 for AA3003-O are found out by using a genetic algorithm in Matlab optimization toolbar and the results are shown in tables 15 and 16. Also the predated anisotropy values through different directions as a result of applying these two yield functions are shown in figure 6 and the predicted yield surfaces are shown in figure 7 as well.

Table 15. BBC2008 coefficients for aluminum alloy AA3003-O.

K	s	w	$l_1^{(1)}$	$l_2^{(1)}$	$m_1^{(1)}$	$m_2^{(1)}$	$m_3^{(1)}$
4	2	1.2247	0.616	0.546	0.56	0.696	0.586
$n_1^{(1)}$	$n_2^{(1)}$	$n_3^{(1)}$	$l_1^{(2)}$	$l_2^{(2)}$	$m_1^{(2)}$	$m_2^{(2)}$	$m_3^{(2)}$
0.481	0.456	-0.003	-0.319	0.031	0.399	0.858	0.2338
$n_1^{(2)}$	$n_2^{(2)}$	$n_3^{(2)}$					
0.184	0.151	0.429					

Table 16. Yld2011 coefficients for aluminum alloy AA3003-O.

c'_{12}	c'_{13}	c'_{21}	c'_{23}	c'_{31}	c'_{32}	c'_{44}	c'_{55}	c'_{66}
0.314	1.116	0.877	0.58	1.066	1.312	1	1	0.811
c''_{12}	c''_{13}	c''_{21}	c''_{23}	c''_{31}	c''_{32}	c''_{44}	c''_{55}	c''_{66}
-0.328	1.512	0.726	0.556	-1.057	0.68	1	1	0.728

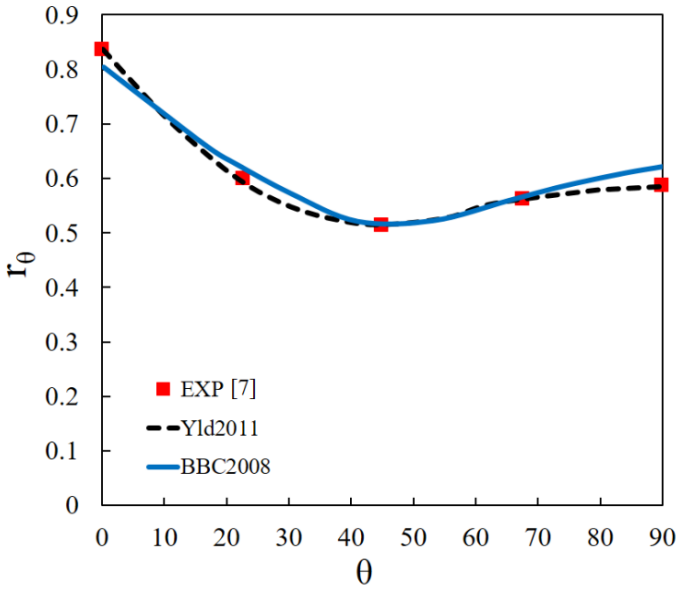

Fig. 6. The predicted experimental directional r-values for alloy AA3003-O.

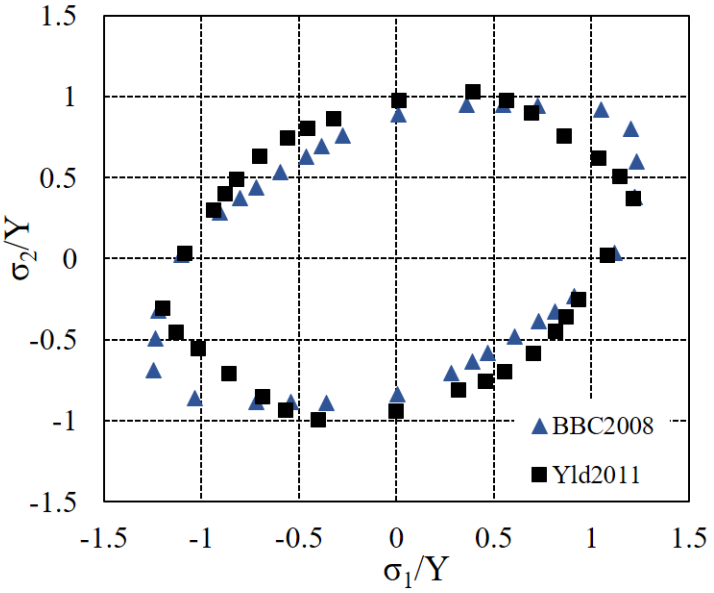

Fig. 7. The predicted yield surfaces in σ_{11}, σ_{22} space where the σ_{12}=0 for Alloy AA3003-O.

The forming limit diagram of this alloy have been considered under the effect of these yield functions and compared with experimental results. Also, the voce hardening law has been used and the parameters of this hardening law are A=199.15, B=91.11 and C=8.93 [7]. Figure 8 shows the schematic results. Also performances of Yld2011 and BBC2008 yield functions in predicting FLD are comparing to each other according to equation (48) listed in table 17. As it is observed, both yield functions predict almost the same value for the tension-compression region but in the right-hand side, BBC2008 predicts more matching results with experimental data.

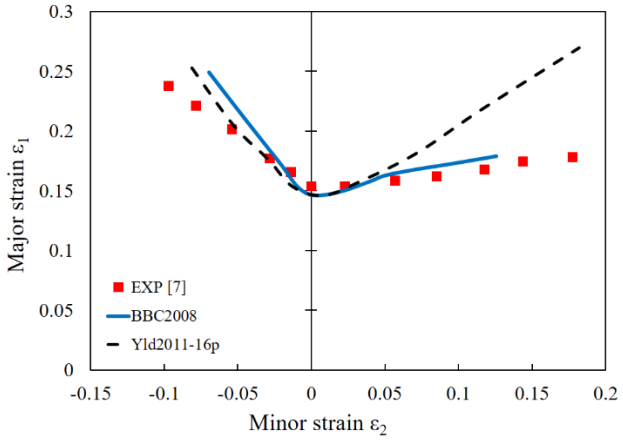

Fig. 8. The predicted FLDs for aluminum alloy AA3003-O.

Table 17. The performance of different yield functions in predicting FLD of AA3003-O (in three strain ratios).

	BBC2008	Yld2011
-1/3	14	5
0	4	4
1	3	>30

5- Conclusion

In this paper, the effect of various developed yield functions were applied to consider the anisotropy of aluminum alloys and to find out their capabilities in predicting anisotropy of metals. Forming limit diagrams of these alloy generated refer to the M-K model and the results were compared with experimental ones.

Forming limit diagrams for AA5754, AA3104-H19, AA5042 and AA2090 are gained by different yield criteria such as BBC2008, Punkett2008, soare2008 and Yld2011 using available coefficients of these yield functions in literatures [8,13,17,22] and voce hardening law.

- Comparing the results according to these developed yield functions for aluminum alloy 2090-T3 shows that all advanced yield functions correctly anticipate the overall trend but in the left side of the curve, predicted results by Yld2011 are better matched with experimental data.
- Forming limit of AA5754 is obtained based on Plunkett yield criterion. The remarkable difference between the theoretical prediction curve and experimental data can be observed in the tension-compression strain states described in the left-hand side of the FLD, but it predicts right-hand side of the FLD with good accuracy.
- Analyzing the FLDs for AA5042-H2 which gained by using Plunkett2008 and BBC2008 shows that, Plunkett 2008 predicted the higher level of FLD than BBC.
- For AA3003-O coefficients of BBC2008 and Yld2011 are found out using minimization of error function through genetic algorithm in Matlab optimization toolbar. Conformity of predicted directional r-values with experimental ones affirm the accuracy of them.
- Forming limit diagram of AA3003-O are predicted by BBC2008 and Yld2011 and compared with experimental data. Both yield functions predict almost the same value for tension-compression region but in right-hand side, BBC2008 predicts results with better accuracy.

References

[1] A. Assempour, R. Hashemi, K. Abrinia, M. Ganjiani, E. Masoumi, “A methodology for prediction of forming limit stress diagrams considering the strain path effect”, Computational materials science, vol. 45, no. 2, pp. 195-204, 2009.

[2] A. Assempour, A.R. Safikhani, R. Hashemi, “An improved strain gradient approach for determination of deformation localization and forming limit diagrams”, Journal of Materials Processing Technology, vol. 209, no. 4, pp. 1758-1769, 2009.

[3]Z. Marciniak and K. Kuczynski, “Limit strains in the processes of stretch-forming sheet metal,” International journal of mechanical sciences, vol. 9, no. 9, pp. 609IN1613–612IN2620, 1967.

[4] R. Hashemi, K. Abrinia, “Analysis of the extended stress-based forming limit curve considering the effects of strain path and through-thickness normal stress”, Materials and Design, vol. 54, pp. 670-677, 2014.

[5] M. Butuc, D. Banabic, A. B. da Rocha, J. Gracio, J. F. Duarte, P. Jurco, and D. Comsa, “The performance of yld96 and bbc2000 yield functions in forming limit prediction,” Journal of materials processing technology, vol. 125, pp. 281–286, 2002.

[6] M. Ganjiani and A. Assempour, “An improved analytical approach for determination of forming limit diagrams considering the effects of yield functions,” Journal of materials processing technology, vol. 182, no. 1,pp. 598–607, 2007.

[7] S. Ahmadi, A. Eivani, and A. Akbarzadeh, “An experimental and theoretical study on the prediction of forming limit diagrams using new bbc yield criteria and m–k analysis,” Computational Materials Science, vol. 44, no. 4, pp. 1272–1280, 2009.

[8] J.-H. Yoon, O. Cazacu, J. W. Yoon, and R. E. Dick, “Earing predictions for strongly textured aluminum sheets,” International journal of mechanical sciences, vol. 52, no. 12, pp. 1563–1578, 2010.

[9] A. Rezaee-Bazzaz, H. Noori, and R. Mahmudi, “Calculation of forming limit diagrams using hill’s 1993 yield criterion,”

International Journal of Mechanical Sciences, vol. 53, no. 4, pp. 262–270, 2011.
[10]P. Dasappa, K. Inal, and R. Mishra, "The effects of anisotropic yield functions and their material parameters on prediction of forming limit diagrams," International Journal of Solids and Structures, vol. 49, no. 25, pp. 3528–3550, 2012.
[11] X. Li, N. Song, G. Guo, and Z. Sun, "Prediction of forming limit curve (flc) for al–li alloy 2198-t3 sheet using different yield functions," Chinese Journal of Aeronautics, vol. 26, no. 5, pp. 1317–1323, 2013.
[12] S. Panich, F. Barlat, V. Uthaisangsuk, S. Suranuntchai, and S. Jirathearanat, "Experimental and theoretical formability analysis using strain and stress based forming limit diagram for advanced high strength steels," Materials & Design, vol. 51, pp. 756–766, 2013.
[13] H. Aretz and F. Barlat, "New convex yield functions for orthotropic metal plasticity," International Journal of non-linear mechanics, vol. 51, pp. 97–111, 2013.
[14] S. Panich and V. Uthaisangsuk, "Effects of anisotropic yield functions on prediction of forming limit diagram for ahs steel," in Key Engineering Materials, vol. 622. Trans Tech Publ, 2014, pp. 257–264.
[15] R. Hill, "A theory of the yielding and plastic flow of anisotropic metals," in Proceedings of the Royal Society of London A: Mathematical, Physical and Engineering Sciences, vol. 193, no. 1033. The Royal
Society, 1948, pp. 281–297.
[16] R. W. Logan and W. F. Hosford, "Upper-bound anisotropic yield locus calculations assuming¡ 111¿-pencil glide," International Journal of Mechanical Sciences, vol. 22, no. 7, pp. 419–430, 1980.
[17] D.-S. Comsa and D. Banabic, "Plane-stress yield criterion for highly-anisotropic sheet metals," Numisheet 2008, Interlaken, Switzerland, pp.43–48, 2008.
[18] S. Soare, J. W. Yoon, and O. Cazacu, "On the use of homogeneous polynomials to develop anisotropic yield functions with applications to sheet forming," International Journal of Plasticity, vol. 24, no. 6, pp.
915–944, 2008.
[19] B. Plunkett, O. Cazacu, and F. Barlat, "Orthotropic yield criteria for description of the anisotropy in tension and compression of sheet metals," International Journal of Plasticity, vol. 24, no. 5, pp. 847–866, 2008.
[20] R. Zhang, Sh. Zhutao, L. Jianguo, "A review on modelling techniques for formability prediction of sheet metal forming," International Journal of Lightweight Materials and Manufacture, 2018.
[21] E. Voce, "The relationship between stress and strain for homogeneous deformation," J Inst Met, vol. 74, pp. 537–562, 1948.
[22] K. Inal, R. K. Mishra, and O. Cazacu, "Forming simulation of aluminum sheets using an anisotropic yield function coupled with crystal plasticity theory," International Journal of Solids and Structures, vol. 47, no. 17, pp. 2223–2233, 2010.
[23] S. Soare and D. Banabic, "A note on the mk computational model for predicting the forming limit strains," International Journal of Material Forming, vol. 1, no. 1, pp. 281–284, 2008.
[24] D. Banabic, O. Cazacu, F. Barlat, D. Comsa, S. Wagner, and K. Siegert, "Description of anisotropic behaviour of aa3103-0 aluminium alloy using two recent yield criteria," in Journal de Physique IV (Proceedings), vol. 105. EDP sciences, 2003, pp. 297–304.
[25] D. Banabic, H. Aretz, D. Comsa, and L. Paraianu, "An improved analytical description of orthotropy in metallic sheets," International Journal of Plasticity, vol. 21, no. 3, pp. 493–512, 2005.
[26] J. H. Holland, Adaptation in natural and artificial systems: an introductory analysis with applications to biology, control, and artificial intelligence. U Michigan Press, 1975.
[27] R. Safdarian, "Forming limit diagram prediction of 6061 aluminum by GTN damage model," Mechanics & Industry, Vol. 19, Issue 2, pp. 202-214, 2018.